AGU ADVANCING EARTH AND SPACE SCIENCE

Geophysical Research Letters

RESEARCH LETTER
10.1029/2020GL088153

Key Point:
- Changes in moisture transport path length to southwestern Scandinavia preceded local summer warming during deglaciation

Supporting Information:
- Supporting Information S1

Correspondence to:
O. C. Cowling,
owencowl@buffalo.edu

Citation:
Cowling, O. C., Thomas, E. K., Svendsen, J. I., Mangerud, J., Vasskog, K., & Haflidason, H. (2020). Northward shifts in the polar front preceded Bølling and Holocene warming in southwestern Scandinavia. *Geophysical Research Letters*, *47*, e2020GL088153. https://doi.org/10.1029/2020GL088153

Received 30 MAR 2020
Accepted 22 JUN 2020
Accepted article online 8 JUL 2020

Northward Shifts in the Polar Front Preceded Bølling and Holocene Warming in Southwestern Scandinavia

O. C. Cowling[1], E. K. Thomas[1], J. I. Svendsen[2,3], J. Mangerud[2,3], K. Vasskog[4,3], and H. Haflidason[2,3]

[1]Department of Geology, University at Buffalo, Buffalo, NY, USA, [2]Department of Earth Science, University of Bergen, Bergen, Norway, [3]Bjerknes Centre for Climate Research, Bergen, Norway, [4]Department of Geography, University of Bergen, Bergen, Norway

Abstract The last deglaciation in northern Europe provides an opportunity to study the hydrologic component of abrupt climate shifts in a region with complex interactions between ice sheets and oceanic and atmospheric circulation. We use leaf wax hydrogen isotopes (δ^2H) to reconstruct summer precipitation δ^2H and aridity in southwestern Norway from 15.8 to 11.5 ka. We identify transitions to a more proximal moisture source before the ends of Heinrich Stadial 1 and the Younger Dryas, prior to local warming and increased primary productivity in both instances. We infer these changes in moisture delivery to southwestern Norway to be a response to northward shifts in the polar front caused by warm water intrusion into the North Atlantic, which preceded abrupt warming in the circum-North Atlantic. These results suggest that moisture transport pathways shift northward as warm surface ocean water reaches higher latitudes in the North Atlantic.

Plain Language Summary The end of the last glacial maximum (~22,000 to 11,600 years ago) in northern Europe contains two particularly abrupt warming events that occurred around 14,600 and 11,600 years ago. These past warming events provide an opportunity to study changes in precipitation and other aspects of hydrology during abrupt temperature increases. We use the ratio of stable isotopes of hydrogen in leaf waxes preserved in lake sediments to reconstruct changes in the transport path length of summer precipitation in southwestern Norway during the Lateglacial 15,800 to 11,600 years ago. We identify changes in precipitation hydrogen isotopes that indicate moisture started coming from sources closer to Norway before this region warmed at the entrance to the Bølling interstadial approximately 14,600 as well as the start of the Holocene 11,600 years ago. We infer these changes in moisture delivery to southwestern Norway to be a response to northward shifts in the polar front caused by sea ice retreat and warm water moving into the North Atlantic, which preceded abrupt terrestrial warming in the circum-North Atlantic. These results suggest that moisture transport pathways shift northward as warmer surface water reaches higher latitudes in the North Atlantic.

1. Introduction

The response of hydrologic conditions (i.e., precipitation moisture source and seasonality and humidity) to abrupt warming is an important component to understanding past climatic changes and for predicting future changes. Northern Europe during the last deglaciation is ideal for studying the hydrological response to complex climate system interactions during abrupt events, as multiple warming and cooling events between the Last Glacial Maximum and the Holocene directly impacted this region (Eldevik et al., 2014). These events involved complex interactions between sea and land ice, ocean circulation, and the positioning of atmospheric fronts (Brauer et al., 2008; Buizert et al., 2014; Eldevik et al., 2014; Hughes et al., 2016; McManus et al., 2004). Two episodes of abrupt warming occurred during the last deglaciation: the Heinrich Stadial 1 (HS-1) to Bølling transition (14.6 ka) and the YD to Holocene transition (11.6 ka). These two abrupt warming events took place against different background climate states, with higher atmospheric CO_2, higher Northern Hemisphere (NH) summer insolation, and smaller continental ice sheets during the YD compared to HS-1 (Hughes et al., 2016; Jouzel et al., 2007; Laskar et al., 2004; Svendsen et al., 2004), which may have altered the timing and nature of hydrologic response to these two abrupt warming events.

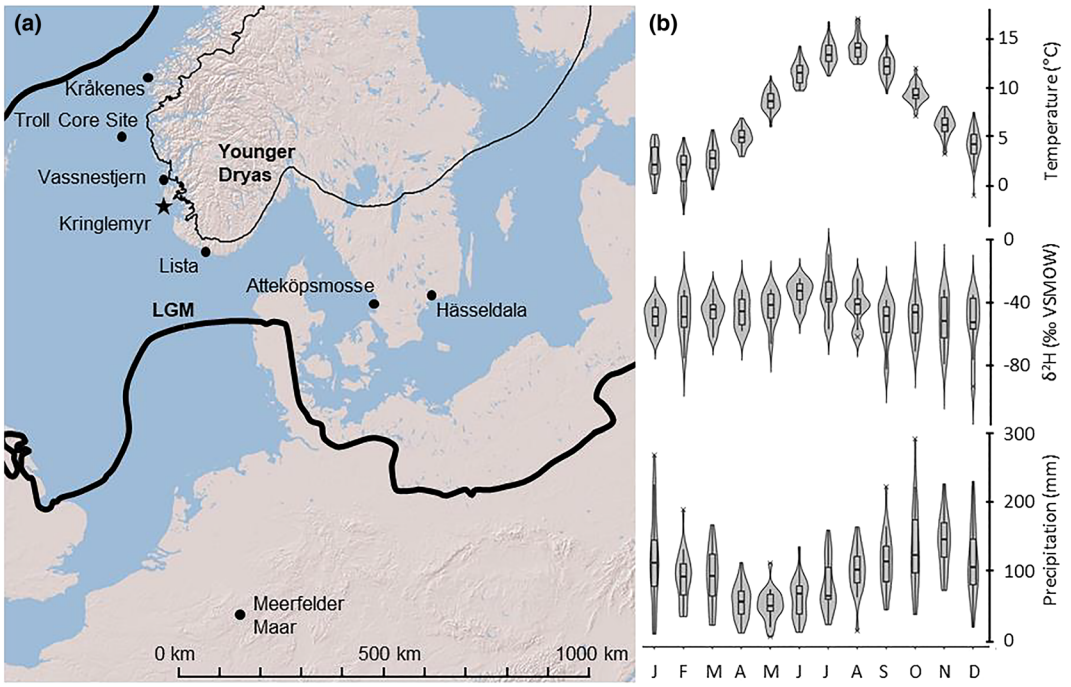

Figure 1. (a) Map of northern Europe showing sites cited in text. The extent of the Scandinavian and British-Irish Ice Sheets at the Last Glacial Maximum (LGM) is indicated by the thick black line (Svendsen et al., 2004). The extent of the Scandinavian Ice Sheet during the Younger Dryas is indicated by the smaller black line (Hughes et al., 2016). (b) Modern seasonality in southwestern Norway as monthly averages. Temperatures and precipitation amount (1943 to 2017, intermittent) are from Utsira (Lawrimore et al., 2011), 25 km northwest of Kringlemyr. Monthly δ^2H data (1961 to 1980) are from Lista (IAEA/WMO, 2018), shown in (a).

Reconstructions of hydrologic changes during the HS-1-Bølling and YD-Holocene transitions could provide insights into the mechanisms controlling hydrological change during abrupt warming and whether boundary conditions influence the hydrological response to warming. Terrestrial records from Scandinavia that span both transitions are rare (Wohlfarth et al., 2018) due to the presence of continental ice sheets over the region prior to the Bølling (Hughes et al., 2016), although there are terrestrial temperature and hydrologic records from south of the ice sheet (Brauer et al., 1999; Heiri et al., 2007). A record in northern Europe suggests that drying lagged cooling into the Younger Dryas, as the westerly wind system migrated southward in response to an expanding sea ice front (Rach et al., 2014), and we might expect the same lag to occur in response to these processes during abrupt warming. We test this hypothesis with a leaf wax hydrogen isotope (δ^2H_{wax}) record from Kringlemyr, an infilled paleolake on Karmøy, southwestern Norway (Figure 1a). The lacustrine record of this isolation basin begins at 15.8 ka (Vasskog et al., 2019) and spans the transitions at the end of HS-1 and the YD, presenting an opportunity to assess the temporal relationship between abrupt warming and hydrology during the last deglaciation.

2. Methods and Approach

2.1. Site Description and Core Details

Karmøy is adjacent to the Norwegian Channel, which became ice free after 18.5 ka, indicated by ^{14}C ages on marine foraminifera (Brendryen et al., 2020; Sejrup et al., 2016). Basal radiocarbon ages from Kringlemyr suggest that the site became ice free shortly before 18 ka (Vasskog et al., 2019), providing a uniquely long-duration sediment record for Scandinavia. Kringlemyr is well positioned to record changes in precipitation sources as a result of repositioning of the polar front and variable Atlantic Meridional Overturning Circulation intensity, as it lies near sea level in the path of prevailing westerly winds on the Norwegian Sea coast.

Core KGM 507-02 was collected from Kringlemyr in November 2014, using an 11.5 cm diameter piston corer. Three overlapping core sections provide undisturbed sediments spanning 455 to 887 cm depth below the surface of the modern peat bog. The lowest part of the core consists of marine sediments that transitioned to lacustrine sediments (646 cm) after the outlet sill of the basin was raised above sea level around 16 ka, indicated by a shift from marine to freshwater phytoplankton at that depth (Vasskog et al., 2019). Lithostratigraphic transitions in the lacustrine portion of Core KGM 507-02, discussed more fully in Vasskog et al. (2019), show a similar pattern to other late-glacial lake sediments in the region (Krüger et al., 2011; Lohne et al., 2004, 2007). Our age-depth model (supporting information Figures S1 and S2 and Text S1) is based on the age-depth model presented by Vasskog et al. (2019), restricted to the lacustrine portion of the record (646–480 cm) and incorporates two additional radiocarbon ages at 622.3 and 581.3 cm (Table S1). Median 2σ age uncertainty for the data presented here is $\pm$147 years, with a maximum of $\pm$256 years and a minimum of $\pm$109 years (Blaauw, 2010; Reimer et al., 2013).

We collected 0.5 cm thick subsamples within the lacustrine sediments for compound-specific stable isotope (δ^2H_{wax}) analysis. Our δ^2H_{wax} record spans 15.8 to 11.5 ka at approximately 100 year resolution, and each sample integrates between 5 and 30 years of sedimentation, with a median of 15 years. Detailed methods are available in Text S2.

2.2. Leaf Wax δ^2H Seasonality

Terrestrial (C_{28}) and aquatic (C_{22}) *n*-alkanoic acid δ^2H reflect the δ^2H value of source water (Thomas et al., 2020), with a biosynthetic offset that is generally constant for a given plant community (Daniels et al., 2017; Sachse et al., 2012). Changes in the relative abundance of plant growth forms (i.e., grasses vs. shrubs) within a catchment can cause changes to δ^2H_{wax} due to differences in biosynthetic fractionation; however, the timing of δ^2H_{wax} changes at Kringlemyr is asynchronous with plant community changes as recorded by pollen in nearby Liastemmen (Paus, 1989), and we do not attempt a pollen-based correction of our δ^2H_{wax} data (Text S3) (Feakins, 2013; Inglis et al., 2020; McFarlin et al., 2019). The δ^2H of water in lakes with residence times less than 6 months is similar to the δ^2H of precipitation during any given season (Cluett & Thomas, 2020; Thomas et al., 2020). Furthermore, the low amplitude of modern seasonal δ^2H_{precip} in southwestern Norway (Figure 1b) (IAEA/WMO, 2018) suggests that plant source water δ^2H would not be strongly impacted if winter precipitation persisted in lake or soil water into the growing season. However, the amplitude of seasonal variation in δ^2H_{precip} may have increased during HS-1 and the YD due to colder winter conditions. We estimate that the residence time of Kringlemyr is less than 6 months (Text S4), meaning that Kringlemyr lake water δ^2H primarily reflects summer precipitation δ^2H during the growing season. Thus, δ^2H_{C22} at Kringlemyr primarily reflects growing season (summer) precipitation δ^2H, which reflects local condensation temperature and the transport history of atmospheric water vapor (Dansgaard, 1964), with some contribution from winter precipitation during HS-1 and the YD. δ^2H_{C28} also reflects summer precipitation δ^2H, plus evaporative enrichment (Kahmen et al., 2013; Sachse et al., 2012). Since both terrestrial and aquatic waxes likely reflect the same source water (e.g., summer precipitation), the calculated offset between δ^2H_{C28} and δ^2H_{C22} ($\varepsilon_{t\text{-}a}$) primarily indicates the magnitude of evaporative enrichment in terrestrial plants, which is inversely related to local relative humidity (Rach et al., 2017; Thomas et al., 2020).

3. Results and Interpretation

3.1. Aquatic Leaf Wax δ^2H at Kringlemyr Reflects Moisture Transport History

Prior to 14.8 ka, primary productivity was low, as indicated by low loss on ignition (LOI) (Vasskog et al., 2019) and low C_{28} *n*-alkanoic acid concentrations in Kringlemyr (Figure 2e) and predominantly reworked and long-distance-transported pollen found at nearby Liastemmen (Paus, 1989). However, freshwater green algae were abundant in Kringelmyr sediments prior to 14.8 ka (Vasskog et al., 2019). We therefore infer that C_{28} *n*-alkanoic acids were partially sourced from aquatic organisms, with relatively limited contributions from terrestrial vegetation (Figure S3) during this interval (van Bree et al., 2018). Prior to 14.8 ka, δ^2H_{C28} does not reliably represent the isotopic composition of terrestrial plant source water, and we therefore restrict our interpretations of δ^2H_{C28} and $\varepsilon_{t\text{-}a}$ after 14.8 ka (Text S5). Aquatic mosses, which are present as macrofossils in this portion of the core (Vasskog et al., 2019), are the most likely source of C_{22} *n*-alkanoic

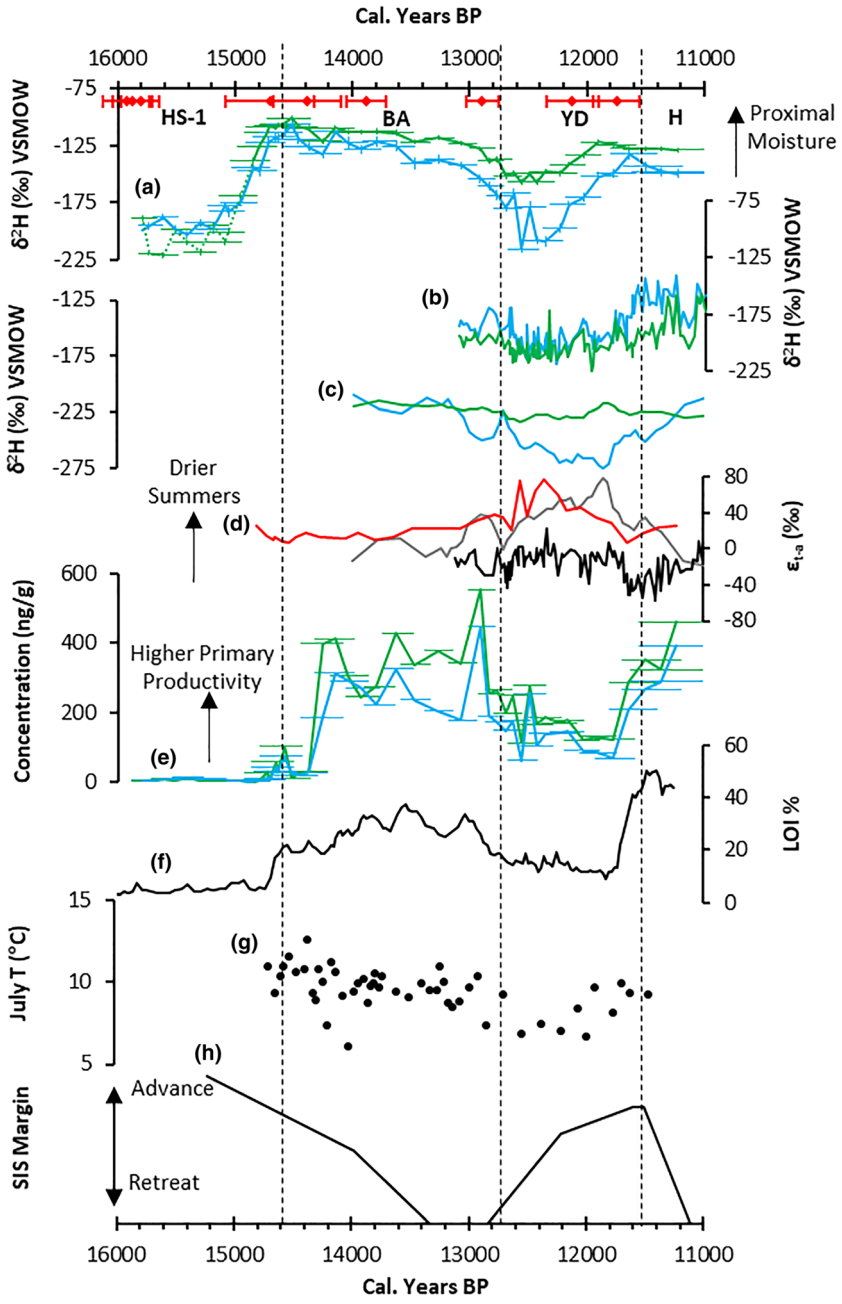

Figure 2. (a) δ^2H_{wax} of C_{22} (blue) and C_{28} (green) fatty acids (‰, VSMOW) from Kringlemyr. (red symbols) Calibrated ^{14}C ages with 2σ uncertainty. (b) δ^2H of C_{23} *n*-alkanes (blue) and C_{29} *n*-alkanes (green) from Meerfelder Maar (Rach et al., 2014). (c) δ^2H_{wax} of C_{21} *n*-alkanes (blue) and amount-weighted δ^2H of $C_{27\text{-}29\text{-}31}$ *n*-alkanes (green) from Hässeldala (Muschitiello et al., 2015). (d) Offset of δ^2H_{C28} relative to δ^2H_{C22} fatty acids from Kringlemyr (red) and equivalent comparisons from Meerfelder Maar (black) and Hässeldala (gray). (e) Sedimentary concentration of C_{22} (blue) and C_{28} (green) fatty acids. C_{22} concentration is magnified 10X. Horizontal error bars in (a) and (e) show 2σ age uncertainty for each sample. (f) Loss on ignition as % of dry sediment mass (Vasskog et al., 2019). (g) July temperature reconstructed from pollen assemblages at Vassnestjern (Karlsen, 2009). (h) Relative position of the Scandinavian Ice Sheet margin in southwestern Norway (Mangerud et al., 2017). Vertical dashed lines show boundaries between Heinrich Stadial-1, the Bølling-Allerød, the Younger Dryas, and the Holocene (Lohne et al., 2013, 2014).

acids throughout the record (Thomas et al., 2020) and may be an important source of C_{28} *n*-alkanoic acids prior to 14.8 ka. Thus, we interpret δ^2H_{C22} to reflect lake water δ^2H composition during the entire record presented here.

We interpret δ^2H_{C22} at Kringlemyr as primarily reflecting changes in summer moisture transport history and $\varepsilon_{t\text{-}a}$ as evaporative enrichment of terrestrial plant leaf water during the growing season, which is primarily controlled by summer relative humidity (Rach et al., 2017; Thomas et al., 2020). Some temperature reconstructions (Figure 2g) and modeling results indicate that summer cooling during the YD was minor (~2°C) in southwestern Norway (Denton et al., 2005; Karlsen, 2009; Schenk et al., 2018), with recent work providing evidence for warm summers and enhanced seasonality during the YD (Schenk et al., 2020). Yet the growth of cirque glaciers, complete deforestation, and the readvancement of the Scandinavian Ice Sheet point to a larger summer temperature depression (Birks et al., 2000; Larsen & Stalsberg, 2004; Lohne et al., 2012; Mangerud et al., 2017; Paus, 1989). In either case, the decrease of 50‰ in δ^2H_{C22} early in the YD (Figure 2a) would require an implausible decrease in summer temperatures of nearly 10°C, based on the global condensation temperature-δ^2H relationship of 5.6‰ $°C^{-1}$ (Dansgaard, 1964).

Changes in temperature at the moisture source location are also insufficient to explain the ^2H depletion in δ^2H_{C22}, as the δ^2H of water vapor evaporated from the ocean at constant relative humidity only decreases by ~1‰ $°C^{-1}$ (Majoube, 1971). A decrease in North Atlantic SST of approximately 5°C during the YD (Kroon et al., 1997) therefore would only result in approximately 5‰ ^2H depletion. The majority of the 50‰ decrease in δ^2H_{C22} from the Allerød to the YD thus primarily reflects a change in the transport path of moisture reaching southwestern Norway. Specifically, we interpret this 50‰ change to indicate a greater proportion of moisture from distal, low latitude sources, which would have experienced ^2H distillation during transport and have ^2H-depleted values prior to reaching southwestern Norway. This is consistent with interpretations of precipitation isotopes and moisture source regions in high latitude environments such as Greenland and Alaska (Klein et al., 2015; Nusbaumer et al., 2019; Putman et al., 2017; Sime et al., 2013; Thomas et al., 2018). The Kringlemyr $\varepsilon_{t\text{-}a}$ record, which we interpret to primarily represent summer relative humidity (Rach et al., 2017), suggests that driest conditions prevailed in southwestern Norway early in the YD between 12.7 and 12.3 ka when δ^2H_{C22} is most ^2H depleted (Figure 2d). Enhanced seasonality during stadials (Schenk et al., 2020) would result in more depleted winter precipitation relative to modern and reduced summer precipitation. This could explain some of the observed depletion in δ^2H_{C22} during the YD and HS-1, as well as the increased $\varepsilon_{t\text{-}a}$ during the YD. While seasonality likely influences our record, it would not produce the observed trends in δ^2H_{C28}, which reflect summer precipitation isotopes yet have a muted trend similar to δ^2H_{C22}. This suggests that both δ^2H_{C22} and δ^2H_{C28} primarily reflect summer precipitation isotopes, which we mainly interpret as changes in moisture transport distance, particularly outside of stadials when seasonality was less pronounced.

4. Discussion

4.1. Comparison to Regional δ^2H_{wax} Records

The transition at Kringlemyr toward higher δ^2H_{C22} and δ^2H_{C28} values between 12.3 and 11.8 ka primarily reflects a northward shift of the polar front and the reduction of summer pressure anomalies over northwestern Europe (Schenk et al., 2018), resulting in more humid, enriched vapor masses reaching southwestern Scandinavia. This gradual shift in moisture transport to Kringlemyr matches reasonably well to the wax δ^2H record from Meerfelder Maar in Germany (Figures 1 and 2b) (Rach et al., 2014). The Meerfelder Maar record is interpreted to reflect generally colder and snowier conditions early in the YD in northern Europe followed by warmer and wetter periods due to oscillations in the zonal position of the westerlies from 12.26 to 11.67 ka.

Leaf-wax isotope reconstructions from southern Sweden at Hässeldala (Figures 1 and 2c) show patterns of change during the YD that largely reflect the influence of meltwater from the Scandinavian Ice Sheet on the isotopic composition of North Sea surface water (Muschitiello et al., 2015; Wohlfarth et al., 2018). The minimum δ^2H_{wax} values at Hässeldala occur several hundred years later than at Kringlemyr. While glacial meltwater also likely had some influence on δ^2H_{precip} at Kringlemyr, the mismatch in timing suggests that it was not the primary factor. Kringlemyr may have been more strongly influenced by changes in the position of the polar front than Hässeldala due to its coastal location on the windward side of the Scandinavian Ice Sheet. Differences in the timing of hydrologic changes between southwestern Norway and southern Sweden show the potential for precipitation isotope variability even within a relatively small geographic region. These regional differences in timing also highlight the influence of the Scandinavian Ice sheet on

climate in Northern Europe during the deglaciation via its impact on atmospheric circulation and surface water conditions in the North Sea (Muschitiello et al., 2015; Schenk et al., 2018; Wohlfarth et al., 2018).

In both Germany and southern Sweden, terrestrial wax records show muted changes during the YD relative to aquatic waxes, similar to the pattern seen at Kringlemyr, and trends in terrestrial δ^2H_{wax} generally agree between sites (Figure 2). However, the magnitude of changes in terrestrial and aquatic δ^2H_{wax} at Kringlemyr is larger than at Meerfelder Maar and Hässeldala. Those sites were not adjacent to the coast (as Kringlemyr is) during the late glacial, so the changes may appear amplified at Kringlemyr due to the large contrast between a strong seasonal cycle during stadials and an almost absent seasonal cycle in δ^2H_{precip} during interstadials. Trends in $\varepsilon_{t\text{-}a}$ broadly agree between the three sites, with higher values during the YD indicating drier conditions at all three sites. This suggests that increased aridity during the YD was a regional signal common to this part of northern Europe.

4.2. Atmospheric Circulation in Southwestern Scandinavia Changed Prior to Abrupt Temperature Changes Between 16 and 11 ka

The shift to higher δ^2H_{C22} values during the second half of the YD at Kringlemyr occurred before substantial temperature increases in southwestern Norway (Figure 3a). Productivity, a qualitative proxy for temperature (Kaplan et al., 2002; Willemse & Törnqvist, 1999) in Kringlemyr's catchment inferred from C_{28} *n*-alkanoic acid concentration, does not increase until 11.7 ka, 400 to 500 years after the increase in δ^2H_{wax} (Figures 3a and 3b). Wax concentrations increase synchronously with and are correlated with LOI (Figure S4) and are measured in the same sediment samples as δ^2H_{wax}, so the lag of productivity behind δ^2H shifts is real and independent of age model uncertainty. While LOI and C_{28} *n*-alkanoic acid concentrations may be altered by variable preservation, the major features in those records are not controlled by preservation (Figure S3). Most temperature reconstructions spanning the YD to Holocene transition in northern Europe and Greenland also show warming around 11.6 ka (Buizert et al., 2014; Eldevik et al., 2014; Lohne et al., 2012, 2014). Thus, our record indicates that moisture source shifts and changes to local aridity during the YD preceded local and regional temperature increases by several hundred years, outside the uncertainty of our age model.

We also infer a summer precipitation source shift from an increase in δ^2H_{C22} beginning around 15.2 ka, which preceded abrupt warming at 14.7 ka on Greenland (Figure 3c) (Buizert et al., 2014). The few available terrestrial temperature reconstructions from northern Europe that span the HS-1 to Bølling transition show increasing summer temperatures around 14.6 ka (Heiri et al., 2007; Wohlfarth et al., 2018). Similar to the YD, the enrichment in δ^2H_{wax} that started at 15.2 ka preceded an increase in terrestrial productivity within Kringlemyr's catchment around 14.8 ka (Figure 3b). We interpret the shift to higher values at 15.2 ka to reflect a northward shift in the westerlies and an attendant decrease in air mass transport path length. The lack of reliable δ^2H_{C28} in Kringlemyr prior to 14.8 ka precludes calculating $\varepsilon_{t\text{-}a}$ during the HS-1 to Bølling transition, and so we cannot directly compare changes in local summer relative humidity at the end of HS-1 to those during the latter half of the YD. Nonetheless, our record suggests that during the deglacial period in southwestern Norway, substantial changes in moisture transport distance consistently preceded abrupt temperature increases by several hundred years.

The inferred depletion in precipitation early in the YD and HS-1 at Kringlemyr was most plausibly caused by an increase in Rayleigh distillation during moisture transport, which indicates an increase in the moisture transport path length to southwestern Norway but may also reflect enhanced seasonality. Depleted precipitation occurred in sync with higher $\varepsilon_{t\text{-}a}$ during the YD, which we interpret as drier summer conditions (Rach et al., 2017) and which is also consistent with a more distal moisture source or reduced poleward moisture from the same source region. The southward extension of perennial sea ice in the North Atlantic during the early YD and HS-1 can explain the apparent greater proportion of distal moisture and dry summers in southwestern Norway (Isarin et al., 1998). Several records in northern Europe suggest that southerly sea ice extent caused a southward shift in the polar front early in the YD (Bakke et al., 2009; Brauer et al., 2008; Eldevik et al., 2014). This shift in the polar front would have reduced westerly moisture transport and increased moisture transport path length to southwestern Norway, in turn causing relatively depleted summer precipitation.

During the YD, after ~12.3 ka, periodic warm water intrusion into the North Atlantic reconstructed by foraminifera and biomarker assemblages in the Labrador Sea (Pearce et al., 2013) and reduced sea ice cover along the eastern margin of the North Atlantic (Müller & Stein, 2014) caused the polar front to shift

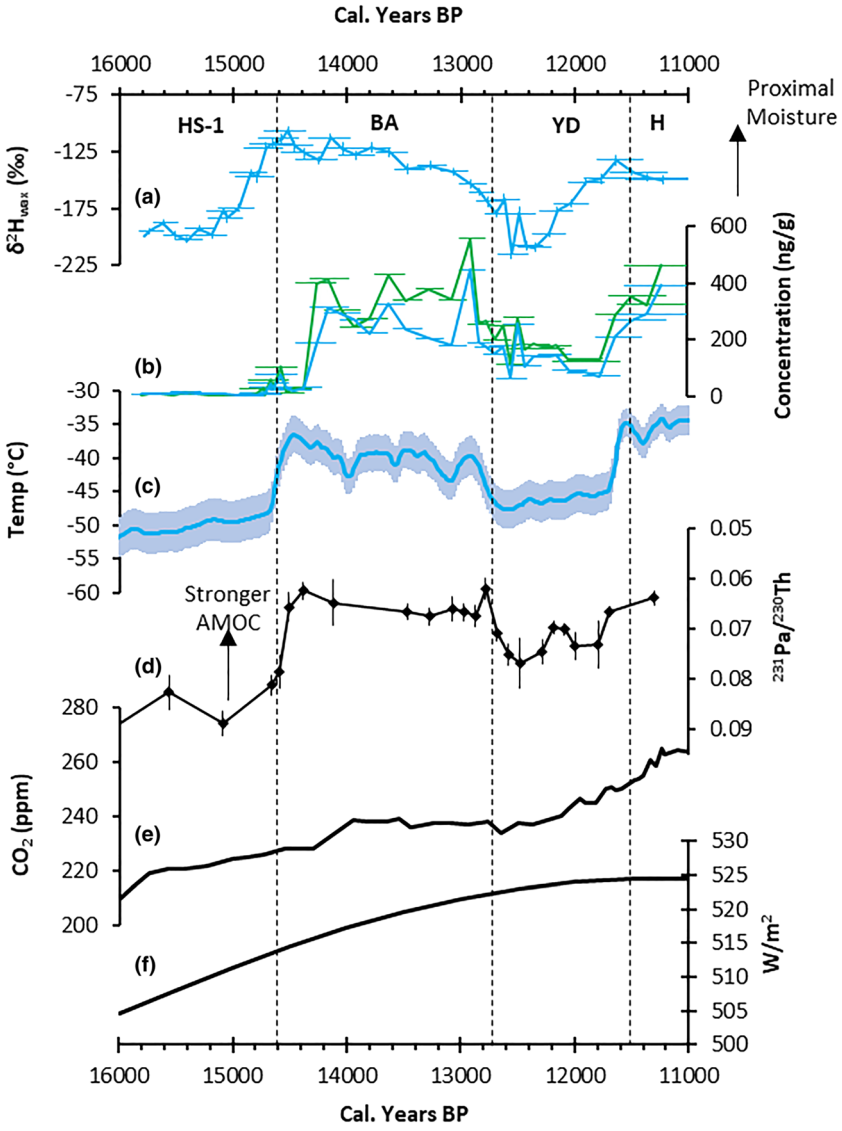

Figure 3. (a) δ^2H_{wax} of C_{22} fatty acids from Kringlemyr. (b) Sedimentary concentration of C_{22} (blue) and C_{28} (green) fatty acids. (c) Composite Greenland temperature reconstruction, layer counted ages before 1950 (Buizert et al., 2014). (d) Pa/Th, a proxy for AMOC intensity (McManus et al., 2004). (e) Mean atmospheric CO_2 concentration from the Epica Dome C ice core record (Jouzel et al., 2007). (f) June 21st insolation at 59°N (Laskar et al., 2004).

northward (Bakke et al., 2009; Baldini et al., 2015; Brauer et al., 2008). This northward shift was intermittent, with the latitudinal position of the polar front oscillating on decadal to centennial time scales, resulting in warming in northern Iberia (Baldini et al., 2015) and latitudinal wind shifts across northern Europe (Bakke et al., 2009; Brauer et al., 2008). During this interval, Kringlemyr δ^2H_{wax} values became more enriched, indicating a decrease in moisture transport distance starting around 12.3 ka, synchronous with the aforementioned sites that record migration of the polar front. The oscillations found later in the YD at Kråkenes and Meerfelder Maar to the north and south, respectively, are not present in our record. However, our sampling frequency is lower during the YD than both Kråkenes and Meerfelder Maar, and our samples integrate longer time intervals than the δ^2H_{wax} record at Meerfelder Maar, so this does not necessarily indicate that those oscillations did not occur in southwestern Norway.

A similar ^2H enrichment in δ^2H_{wax} occurred at Kringlemyr during the end of HS-1 before the start of the Bølling interstadial, which could also be explained by changes in the position of the polar front. Paired foraminifera and pollen from the Iberian margin record complex changes within Heinrich Stadials, showing

wet conditions early in HS-1 followed by drier and slightly warmer conditions later in HS-1, which the authors interpret as a northward shift of the polar front during HS-1 and as early as 17 ka (Naughton et al., 2009, 2016). The northward shift of the polar front may have been caused by northward intrusion of warm surface water from the subtropical North Atlantic, as indicated by lower abundance of *Neogloboquadrina pachyderma* off the Iberian margin (Eynaud et al., 2009). The large delay between the hydrological changes at the Iberian margin (17 ka) and at Kringlemyr (15.2 ka) suggests that additional factors were at work during the end of HS-1.

The similar timing of sea ice retreat and the onset of hydrological change at Kringlemyr point to this latitudinal difference in timing being affected by sea ice extent. There is evidence for warm surface water entering the Norwegian sea by at least 14.8 ka (Mangerud, 1977; Mangerud et al., 2017; Mangerud & Svendsen, 2018) and retreat of the seasonal sea ice front northward along the Norwegian coast around 15 ka (Rochon et al., 1998; Wiig, 2019), at the same time or slightly after the inferred moisture transport changes at Kringlemyr. In this part of western Norway, a significant deglaciation of the Boknafjord region occurred at least 1,000 years before the onset of the Bølling (Vasskog et al., 2019). Additional marine evidence from near Svalbard confirms a reduction in sea ice extent after 16.3 ka and shows progressively increasing primary productivity from 16.3 ka to the onset of the Bølling (Köseoğlu et al., 2019). There is substantial evidence for multiple meltwater pulses during HS-1 and enhanced sea ice export from the Arctic until the onset of the Bølling (Hodell et al., 2017; Thornalley et al., 2011), which may have delayed the northward migration of the polar front. We infer that the lag between the polar front leaving its southernmost position around Iberia and reaching southwestern Scandinavia before the end of HS-1 is caused by the interplay between gradual migration of warm water northward and the prolonged influence of meltwater in the subpolar North Atlantic during the end of HS-1. Based on the strong similarities of both the HS-1 and YD transitions in our δ^2H_{wax} record and the corroborating evidence of other paleoclimate records, we suggest that Kringlemyr records northward shifts of the polar front and possibly less extreme seasonality before the warming that marks the start of the Bølling.

The shift in moisture transport prior to local temperature increases inferred during the transitions into the Bølling-Allerød and Holocene suggests a common mechanism. There is evidence that despite cold winter conditions in the North Atlantic, HS-1 and the YD experienced consistent increases in global temperature, particularly in the Southern Hemisphere (Bereiter et al., 2018; Shakun et al., 2012) as a result of rising NH summer insolation and atmospheric CO_2 through the deglacial interval (Jouzel et al., 2007; Laskar et al., 2004) (Figures 3e and 3f). At the onset of HS-1 and the YD, input of freshwater from melting ice sheets may have contributed to a reduced Atlantic Meridional Overturning Circulation and colder NH, along with a southward displacement of sea ice and the polar front (Hodell et al., 2017; Thornalley et al., 2010). This resulted in a heat imbalance between the NH and Southern Hemisphere, resulting in increased atmospheric heat transport from the subtropics to the NH (McGee et al., 2014). During both HS-1 and the YD, warm water intrusion into the North Atlantic and Norwegian Seas (Müller & Stein, 2014; Pearce et al., 2013; Thornalley et al., 2011) resulted in reductions to sea ice cover (Köseoğlu et al., 2019; Wiig, 2019) and northward repositioning of the polar front prior to terrestrial NH warming (Bakke et al., 2009; Baldini et al., 2015; Brauer et al., 2008; Eynaud et al., 2009; Naughton et al., 2009). The inferred changes at Kringlemyr are consistent with existing understanding of polar front migration through the deglacial period and provide terrestrial evidence confirming the consistency of this mechanism in southwestern Scandinavia. At the end of the YD and HS-1, the position of the sea ice front and interhemispheric temperature gradients controlled oceanic heat distribution, which in turn controlled the position of the polar front, driving the inferred changes in southwestern Scandinavia. Given current trends of sea ice retreat, there may be corresponding future changes in moisture transport to regions of the Arctic that are currently north of the polar front.

Conflict of Interest

The authors declare that they have no financial conflict of interest related to this research.

Data Availability Statement

Data presented in this publication can be accessed online (https://www.ncdc.noaa.gov/paleo/study/29352).

Acknowledgments

This research was funded by the Research Council of Norway through the project Climate History Along the Arctic Seaboard of Eurasia (CHASE) Project 225415/E10 and the Geological Society of America Graduate Student Research Grant. Dr. Elizabeth Thomas and Owen Cowling are supported by NSF Grant EAR-IF 1652274. We thank Dr. Aage Paus for contributions to this work including pollen data from southwestern Norway and assistance with interpretation of said data, Dr. Jason Briner for comments and assistance during preparation of this manuscript, Dr. Beata Csatho for comments on an early version of this research, and Rienk Smittenberg and Gordon Inglis for constructive reviews.

References

Bakke, J., Lie, Ø., Heegaard, E., Dokken, T., Haug, G. H., Birks, H. H., et al. (2009). Rapid oceanic and atmospheric changes during the Younger Dryas cold period. *Nature Geoscience*, *2*(3), 202–205. https://doi.org/10.1038/ngeo439

Baldini, L. M., McDermott, F., Baldini, J. U. L., Arias, P., Cueto, M., Fairchild, I. J., et al. (2015). Regional temperature, atmospheric circulation, and sea-ice variability within the Younger Dryas event constrained using a speleothem from northern Iberia. *Earth and Planetary Science Letters*, *419*, 101–110. https://doi.org/10.1016/j.epsl.2015.03.015

Bereiter, B., Shackleton, S., Baggenstos, D., Kawamura, K., & Severinghaus, J. (2018). Mean global ocean temperatures during the last glacial transition. *Nature*, *553*(7686), 39–44. https://doi.org/10.1038/nature25152

Birks, H. H., Battarbee, R. W., & Birks, H. J. B. (2000). The development of the aquatic ecosystem at Kråkenes Lake, western Norway, during the late glacial and early Holocene-a synthesis. *Journal of Paleolimnology*, *23*(1), 91–114. https://doi.org/10.1023/A:1008079725596

Blaauw, M. (2010). Methods and code for 'classical' age-modelling of radiocarbon sequences. *Quaternary Geochronology*, *5*(5), 512–518. https://doi.org/10.1016/j.quageo.2010.01.002

Brauer, A., Endres, C., & Negendank, J. F. (1999). Lateglacial calendar year chronology based on annually laminated sediments from Lake Meerfelder Maar, Germany. *Quaternary International*, *61*(1), 17–25. https://doi.org/10.1016/S1040-6182(99)00014-2

Brauer, A., Haug, G. H., Dulski, P., Sigman, D. M., & Negendank, J. F. W. (2008). An abrupt wind shift in western Europe at the onset of the Younger Dryas cold period. *Nature Geoscience*, *1*(8), 520–523. https://doi.org/10.1038/ngeo263

Brendryen, J., Haflidason, H., Yokoyama, Y., Haaga, K. A., & Hannisdal, B. (2020). Eurasian ice sheet collapse was a major source of meltwater pulse 1A 14,600 years ago. *Nature Geoscience*, *13*(5), 363–368. https://doi.org/10.1038/s41561-020-0567-4

Buizert, C., Vasileios, G., Severinghaus, J. P., Feng, H., Lecavalier, B., Kindler, P., et al. (2014). Greenland temperature response to climate forcing during the last deglaciation. *Science Reports*, *345*(6201), 1177–1180. https://doi.org/10.1126/science.1254961

Cluett, A. A., & Thomas, E. K. (2020). Resolving combined influences of inflow and evaporation on western Greenland lake water isotopes to inform paleoclimate inferences. *Journal of Paleolimnology*, *63*(4), 251–268. https://doi.org/10.1007/s10933-020-00114-4

Daniels, W. C., Russell, J. M., Giblin, A. E., Welker, J. M., Klein, E. S., & Huang, Y. (2017). Hydrogen isotope fractionation in leaf waxes in the Alaskan Arctic tundra. *Geochimica et Cosmochimica Acta*, *213*, 216–236. https://doi.org/10.1016/j.gca.2017.06.028

Dansgaard, W. (1964). Stable isotopes in precipitation. *Tellus*, *16*(4), 436–468. https://doi.org/10.1111/j.2153-3490.1964.tb00181.x

Denton, G., Alley, R., Comer, G., & Broecker, W. (2005). The role of seasonality in abrupt climate change. *Quaternary Science Reviews*, *24*(10–11), 1159–1182. https://doi.org/10.1016/j.quascirev.2004.12.002

Eldevik, T., Risebrobakken, B., Bjune, A. E., Andersson, C., Birks, H. J. B., Dokken, T. M., et al. (2014). A brief history of climate—The northern seas from the Last Glacial Maximum to global warming. *Quaternary Science Reviews*, *106*, 225–246. https://doi.org/10.1016/j.quascirev.2014.06.028

Eynaud, F., de Abreu, L., Voelker, A., Schönfeld, J., Salgueiro, E., Turon, J.-L., et al. (2009). Position of the polar front along the western Iberian margin during key cold episodes of the last 45 ka. *Geochemistry, Geophysics, Geosystems*, *10*, Q07U05. https://doi.org/10.1029/2009GC002398

Feakins, S. J. (2013). Pollen-corrected leaf wax D/H reconstructions of northeast African hydrological changes during the late Miocene. *Palaeogeography, Palaeoclimatology, Palaeoecology*, *374*, 62–71. https://doi.org/10.1016/j.palaeo.2013.01.004

Heiri, O., Cremer, H., Engels, S., Hoek, W. Z., Peeters, W., & Lotter, A. F. (2007). Lateglacial summer temperatures in the Northwest European lowlands: A chironomid record from Hijkermeer, the Netherlands. *Quaternary Science Reviews*, *26*(19–21), 2420–2437. https://doi.org/10.1016/j.quascirev.2007.06.017

Hodell, D. A., Nicholl, J. A., Bontognali, T. R. R., Danino, S., Dorador, J., Dowdeswell, J. A., et al. (2017). Anatomy of Heinrich Layer 1 and its role in the last deglaciation. *Paleoceanography*, *32*, 284–303. https://doi.org/10.1002/2016PA003028

Hughes, A. L. C., Gyllencreutz, R., Lohne, Ø. S., Mangerud, J., & Svendsen, J. I. (2016). The last Eurasian ice sheets—A chronological database and time-slice reconstruction, DATED-1. *Boreas*, *45*(1), 1–45. https://doi.org/10.1111/bor.12142

IAEA/WMO. (2018). Global network of isotopes in precipitation. The GNIP database. Retrieved from https://www.iaea.org/services/networks/gnip

Inglis, G. N., Carmichael, M. J., Farnsworth, A., Lunt, D. J., & Pancost, R. D. (2020). A long-term, high-latitude record of Eocene hydrological change in the Greenland region. *Palaeogeography, Palaeoclimatology, Palaeoecology*, *537*, 109378. https://doi.org/10.1016/j.palaeo.2019.109378

Isarin, R. F., Renssen, H., & Vandenberghe, J. (1998). The impact of the North Atlantic Ocean on the Younger Dryas climate in northwestern and central Europe. *Journal of Quaternary Science*, *13*(5), 447–453. https://doi.org/10.1002/(SICI)1099-1417(1998090)13:5%3C447::AID-JQS402%3E3.0.CO;2-B

Jouzel, J., Masson-Delmotte, V., Cattani, O., Dreyfus, G., Falourd, S., Hoffmann, G., et al. (2007). Orbital and millennial Antarctic climate variability over the past 800,000 years. *Science Reports*, *317*(5839), 793–796. https://doi.org/10.1126/science.1141038

Kahmen, A., Schefuß, E., & Sachse, D. (2013). Leaf water deuterium enrichment shapes leaf wax *n*-alkane δD values of angiosperm plants I: Experimental evidence and mechanistic insights. *Geochimica et Cosmochimica Acta*, *111*, 39–49. https://doi.org/10.1016/j.gca.2012.09.003

Kaplan, M. R., Wolfe, A. P., & Miller, G. H. (2002). Holocene environmental variability in southern Greenland inferred from lake sediments. *Quaternary Research*, *58*(2), 149–159. https://doi.org/10.1006/qres.2002.2352

Karlsen, L. C. (2009). Lateglacial vegetation and environment at the mouth of Hardangerfjorden, western Norway. *Boreas*, *38*(2), 315–334. https://doi.org/10.1111/j.1502-3885.2008.00062.x

Klein, E. S., Cherry, J. E., Young, J., Noone, D., Leffler, A. J., & Welker, J. M. (2015). Arctic cyclone water vapor isotopes support past sea ice retreat recorded in Greenland ice. *Scientific Reports*, *5*, 10295. https://doi.org/10.1038/srep10295

Köseoğlu, D., Belt, S. T., & Knies, J. (2019). Abrupt shifts of productivity and sea ice regimes at the western Barents Sea slope from the Last Glacial Maximum to the Bølling-Allerød interstadial. *Quaternary Science Reviews*, *222*, 105903. https://doi.org/10.1016/j.quascirev.2019.105903

Kroon, D., Austin, W. E. N., Chapman, M. R., & Ganssen, G. M. (1997). Deglacial surface circulation changes in the northeastern Atlantic: Temperature and salinity records off NW Scotland on a century scale. *Paleoceanography*, *12*(6), 755–763. https://doi.org/10.1029/97PA02289

Krüger, L. C., Paus, A., Svendsen, J. I., & Bjune, A. E. (2011). Lateglacial vegetation and palaeoenvironment in W Norway, with new pollen data from the Sunnmøre region. *Boreas*, *40*(4), 616–635. https://doi.org/10.1111/j.1502-3885.2011.00213.x

Larsen, E., & Stalsberg, M. K. (2004). Younger Dryas glaciolacustrine rhythmites and cirque glacier variations at Kråkenes, western Norway: Depositional processes and climate. *Journal of Paleolimnology*, *31*(1), 49–61. https://doi.org/10.1023/B:JOPL.0000013282.14240.e5

Laskar, J., Robutel, P., Joutel, F., Gastineau, M., Correia, A. C. M., & Levrard, B. (2004). A long-term numerical solution for the insolation quantities of the Earth. *Astronomy & Astrophysics*, *428*(1), 261–285. https://doi.org/10.1051/0004-6361%3A20041335

Lawrimore, J. H., Menne, M. J., Gleason, B. E., Williams, C. N., Wuertz, D. B., Vose, R. S., & Rennie, J. (2011). An overview of the Global Historical Climatology Network monthly mean temperature data set, version 3. *Journal of Geophysical Research*, *116*(D19). https://doi.org/10.1029/2011jd016187

Lohne, Ø. S., Bondevik, S., Mangerud, J., & Schrader, H. (2004). Calendar year age estimates of Allerød–Younger Dryas sea-level oscillations at Os, western Norway. *Journal of Quaternary Science*, *19*(5), 443–464. https://doi.org/10.1002/jqs.846

Lohne, Ø. S., Bondevik, S., Mangerud, J., & Svendsen, J. I. (2007). Sea-level fluctuations imply that the Younger Dryas ice-sheet expansion in western Norway commenced during the Allerød. *Quaternary Science Reviews*, *26*(17–18), 2128–2151. https://doi.org/10.1016/j.quascirev.2007.04.008

Lohne, Ø. S., Mangerud, J., & Birks, H. H. (2013). Precise ^{14}C ages of the Vedde and Saksunarvatn ashes and the Younger Dryas boundaries from western Norway and their comparison with the Greenland Ice Core (GICC05) chronology. *Journal of Quaternary Science*, *28*(5), 490–500. https://doi.org/10.1002/jqs.2640

Lohne, Ø. S., Mangerud, J., & Birks, H. H. (2014). IntCal13 calibrated ages of the Vedde and Saksunarvatn ashes and the Younger Dryas boundaries from Kråkenes, western Norway. *Journal of Quaternary Science*, *29*(5), 506–507. https://doi.org/10.1002/jqs.2722

Lohne, Ø. S., Mangerud, J., & Svendsen, J. I. (2012). Timing of the younger dryas glacial maximum in western Norway. *Journal of Quaternary Science*, *27*(1), 81–88. https://doi.org/10.1002/jqs.1516

Majoube, M. (1971). Oxygen-18 and deuterium fractionation between water and steam. *Journal de Chimie Physique et de Physico-Chimie Biologique*, *68*(10), 1423–1436. https://doi.org/10.1051/jcp/1971681423

Mangerud, J. (1977). Late Weichselian marine sediments containing shells, foraminifera, and pollen, at Ågotnes, western Norway. *Norsk Geologisk Tidsskrift*, *57*, 23–54.

Mangerud, J., Briner, J. P., Goslar, T., & Svendsen, J. I. (2017). The Bølling-age Blomvåg beds, western Norway: Implications for the Older Dryas glacial re-advance and the age of the deglaciation. *Boreas*, *46*(2), 162–184. https://doi.org/10.1111/bor.12208

Mangerud, J., & Svendsen, J. I. (2018). The holocene thermal maximum around Svalbard, Arctic North Atlantic; molluscs show early and exceptional warmth. *The Holocene*, *28*(1), 65–83. https://doi.org/10.1177/2F0959683617715701

McFarlin, J. M., Axford, Y., Masterson, A. L., & Osburn, M. R. (2019). Calibration of modern sedimentary δ^2H plant wax-water relationships in Greenland lakes. *Quaternary Science Reviews*, *225*, 105978. https://doi.org/10.1016/j.quascirev.2019.105978

McGee, D., Donohoe, A., Marshall, J., & Ferreira, D. (2014). Changes in ITCZ location and cross-equatorial heat transport at the Last Glacial Maximum, Heinrich Stadial 1, and the mid-Holocene. *Earth and Planetary Science Letters*, *390*, 69–79. https://doi.org/10.1016/j.epsl.2013.12.043

McManus, J. F., Francois, R., Gherardi, J.-M., Keigwin, L. D., & Brown-Leger, S. (2004). Collapse and rapid resumption of Atlantic meridional circulation linked to deglacial climate changes. *Nature*, *428*(6985), 834–837. https://doi.org/10.1038/nature02494

Müller, J., & Stein, R. (2014). High-resolution record of late glacial and deglacial sea ice changes in Fram Strait corroborates ice–ocean interactions during abrupt climate shifts. *Earth and Planetary Science Letters*, *403*, 446–455. https://doi.org/10.1016/j.epsl.2014.07.016

Muschitiello, F., Pausata, F. S. R., Watson, J. E., Smittenberg, R. H., Salih, A. A. M., Brooks, S. J., et al. (2015). Fennoscandian freshwater control on Greenland hydroclimate shifts at the onset of the Younger Dryas. *Nature Communications*, *6*, 8939. https://doi.org/10.1038/ncomms9939

Naughton, F., Sánchez Goñi, M. F., Kageyama, M., Bard, E., Duprat, J., Cortijo, E., et al. (2009). Wet to dry climatic trend in north-western Iberia within Heinrich events. *Earth and Planetary Science Letters*, *284*(3–4), 329–342. https://doi.org/10.1016/j.epsl.2009.05.001

Naughton, F., Sanchez Goñi, M. F., Rodrigues, T., Salgueiro, E., Costas, S., Desprat, S., et al. (2016). Climate variability across the last deglaciation in NW Iberia and its margin. *Quaternary International*, *414*, 9–22. https://doi.org/10.1016/j.quaint.2015.08.073

Nusbaumer, J., Alexander, P. M., LeGrande, A. N., & Tedesco, M. (2019). Spatial shift of Greenland moisture sources related to enhanced Arctic warming. *Geophysical Research Letters*, *46*, 14,723–14,731. https://doi.org/10.1029/2019GL084633

Paus, A. (1989). Late Weichselian vegetation, climate, and floral migration at Liastemmen, North Rogaland, south-western Norway. *Journal of Quaternary Science*, *4*(3), 223–242. https://doi.org/10.1002/jqs.3390040304

Pearce, C., Seidenkrantz, M.-S., Kuijpers, A., Massé, G., Reynisson, N. F., & Kristiansen, S. M. (2013). Ocean lead at the termination of the Younger Dryas cold spell. *Nature Communications*, *4*, 1664. https://doi.org/10.1038/ncomms2686

Putman, A. L., Feng, X., Sonder, L. J., & Posmentier, E. S. (2017). Annual variation in event-scale precipitation δ^2H at Barrow, AK, reflects vapor source region. *Atmospheric Chemistry and Physics*, *17*(7), 4627–4639. https://doi.org/10.5194/acp-17-4627-2017

Rach, O., Brauer, A., Wilkes, H., & Sachse, D. (2014). Delayed hydrological response to Greenland cooling at the onset of the Younger Dryas in western Europe. *Nature Geoscience*, *7*(2), 109–112. https://doi.org/10.1038/ngeo2053

Rach, O., Kahmen, A., Brauer, A., & Sachse, D. (2017). A dual-biomarker approach for quantification of changes in relative humidity from sedimentary lipid D/H ratios. *Climate of the Past*, *13*(7), 741–757. https://doi.org/10.5194/cp-13-741-2017

Reimer, P. J., Bard, E., Bayliss, A., Beck, J. W., Blackwell, P. G., Ramsey, C. B., et al. (2013). IntCal13 and Marine13 radiocarbon age calibration curves 0–50,000 years cal BP. *Radiocarbon*, *55*(4), 1869–1887. https://doi.org/10.2458/azu_js_rc.55.16947

Rochon, A., de Vernal, A., Sejrup, H.-P., & Haflidason, H. (1998). Palynological evidence of climatic and oceanographic changes in the North Sea during the last deglaciation. *Quaternary Research*, *49*(2), 197–207. https://doi.org/10.1006/qres.1997.1956

Sachse, D., Billault, I., Bowen, G. J., Chikaraishi, Y., Dawson, T. E., Feakins, S. J., et al. (2012). Molecular paleohydrology: Interpreting the hydrogen-isotopic composition of lipid biomarkers from photosynthesizing organisms. *Annual Review of Earth and Planetary Sciences*, *40*(1), 221–249. https://doi.org/10.1146/annurev-earth-042711-105535

Schenk, F., Bennike, O., Väliranta, M., Avery, R., Björck, S., & Wohlfarth, B. (2020). Floral evidence for high summer temperatures in southern Scandinavia during 15–11 cal ka BP. *Quaternary Science Reviews*, *233*, 106243. https://doi.org/10.1016/j.quascirev.2020.106243

Schenk, F., Väliranta, M., Muschitiello, F., Tarasov, L., Heikkilä, M., Björck, S., et al. (2018). Warm summers during the Younger Dryas cold reversal. *Nature Communications*, *9*(1), 1634. https://doi.org/10.1038/s41467-018-04071-5

Sejrup, H. P., Clark, C. D., & Hjelstuen, B. O. (2016). Rapid ice sheet retreat triggered by ice stream debuttressing: Evidence from the North Sea. *Geology*, *44*(5), 355–358. https://doi.org/10.1130/G37652.1

Shakun, J. D., Clark, P. U., He, F., Marcott, S. A., Mix, A. C., Liu, Z., et al. (2012). Global warming preceded by increasing carbon dioxide concentrations during the last deglaciation. *Nature*, *484*(7392), 49–54. https://doi.org/10.1038/nature10915

Sime, L. C., Risi, C., Tindall, J. C., Sjolte, J., Wolff, E. W., Masson-Delmotte, V., & Capron, E. (2013). Warm climate isotopic simulations: What do we learn about interglacial signals in Greenland ice cores? *Quaternary Science Reviews*, *67*, 59–80. https://doi.org/10.1016/j.quascirev.2013.01.009

Svendsen, J. I., Alexanderson, H., Astakhov, V. I., Demidov, I., Dowdeswell, J. A., Funder, S., et al. (2004). Late Quaternary ice sheet history of northern Eurasia. *Quaternary Science Reviews*, *23*(11-13), 1229–1271. https://doi.org/10.1016/j.quascirev.2003.12.008

Thomas, E. K., Hollister, K. V., Cluett, A. A., & Corcoran, M. C. (2020). Reconstructing Arctic precipitation seasonality using aquatic leaf wax δ^2H in lakes with contrasting residence times. *Paleoceanography and Paleoclimatology*, *35*(7), e2020PA003886. https://doi.org/10.1029/2020PA003886

Thomas, E. K., Castañeda, I. S., McKay, N. P., Briner, J. P., Salacup, J. M., Nguyen, K. Q., & Schweinsberg, A. D. (2018). A wetter Arctic coincident with hemispheric warming 8,000 years ago. *Geophysical Research Letters*, *45*, 10,637–10,647. https://doi.org/10.1029/2018GL079517

Thornalley, D. J. R., Elderfield, H., & McCave, I. N. (2011). Reconstructing North Atlantic deglacial surface hydrography and its link to the Atlantic overturning circulation. *Global and Planetary Change*, *79*(3–4), 163–175. https://doi.org/10.1016/j.gloplacha.2010.06.003

Thornalley, D. J. R., McCave, I. N., & Elderfield, H. (2010). Freshwater input and abrupt deglacial climate change in the North Atlantic. *Paleoceanography*, *25*, PA1201. https://doi.org/10.1029/2009PA001772

van Bree, L. G. J., Peterse, F., van der Meer, M. T. J., Middelburg, J. J., Negash, A. M. D., De Crop, W., et al. (2018). Seasonal variability in the abundance and stable carbon-isotopic composition of lipid biomarkers in suspended particulate matter from a stratified equatorial lake (Lake Chala, Kenya/Tanzania): Implications for the sedimentary record. *Quaternary Science Reviews*, *192*, 208–224. https://doi.org/10.1016/j.quascirev.2018.05.023

Vasskog, K., Svendsen, J., Mangerud, J., Agasøster Haaga, K., Svean, A., & Lunnan, E. M. (2019). Evidence of early deglaciation (18 000 cal a BP) and a postglacial relative sea-level curve from southern Karmøy, south-west Norway. *Journal of Quaternary Science*, *34*(6), 410–423. https://doi.org/10.1002/jqs.3109

Wiig, Ø. (2019). Late Pleistocene and Holocene occurrence of bowhead whales (*Balaena mysticetus*) along the coasts of Norway. *Polar Biology*, *42*(4), 645–656. https://doi.org/10.1007/s00300-019-02460-0

Willemse, N., & Törnqvist, T. (1999). Holocene century-scale temperature variability from West Greenland lake records. *Geology*, *27*(7), 580–584. https://doi.org/10.1130/0091-7613(1999)027%3C0580:HCSTVF%3E2.3.CO;2

Wohlfarth, B., Luoto, T. P., Muschitiello, F., Väliranta, M., Björck, S., Davies, S. M., et al. (2018). Climate and environment in southwest Sweden 15.5-11.3 cal. ka BP. *Boreas*, *47*(3), 687–710. https://doi.org/10.1111/bor.12310